THE JOURNAL OF BIOLOGICAL CHEMISTRY VOL. 287, NO. 11, pp. 8101–8109, March 9, 2012

Glutamate 268 Regulates Transport Probability of the Anion/Proton Exchanger ClC-5*[S]

Received for publication, August 31, 2011, and in revised form, January 18, 2012 Published, JBC Papers in Press, January 20, 2012, DOI 10.1074/jbc.M111.298265

Matthias Grieschat and Alexi K. Alekov[1]

From the Institut für Neurophysiologie, Medizinische Hochschule Hannover, D-30625 Hannover, Germany

Background: ClC transporters undergo transitions between actively transporting and inactive states.
Results: The transport probability and nonlinear capacitances of ClC-5 are regulated by internal pH.
Conclusion: The effects of internal pH on ClC-5 transport depend on the ability of Glu-268 to accept and transmit protons.
Significance: The results provide new insight into the function and regulation of ClC transporters.

The Cl^-/H^+ exchange mediated by ClC transporters can be uncoupled by external SCN^- and mutations of the proton glutamate, a conserved residue at the internal side of the protein. We show here for the mammalian ClC transporter ClC-5 that acidic internal pH led to a greater increase in currents upon exchanging extracellular Cl^- for SCN^-. However, transport uncoupling, unitary current amplitudes, and the voltage dependence of the depolarization-induced activation were not altered by low pH values. Therefore, it is likely that an additional gating process regulates ClC-5 transport. Higher internal $[H^+]$ and the proton glutamate mutant E268H altered the ratio between ClC-5 transport and nonlinear capacitance, indicating that the gating charge movements in ClC-5 arise from incomplete transport cycles and that internal protons increase the transport probability of ClC-5. This was substantiated by site-directed sulfhydryl modification of the proton glutamate mutant E268C. The mutation exhibited small transport currents together with prominent gating charge movements. The charge restoration using a negatively charged sulfhydryl reagent reinstated also the WT phenotype. Neutralization of the charge of the gating glutamate 211 by the E211C mutation abolished the effect of internal protons, showing that the increased transport probability of ClC-5 results from protonation of this residue. S168P (a mutation that decreases the anion affinity of the central binding site) reduced also the internal pH dependence of ClC-5. These results support the idea that protonation of the gating glutamate 211 at the central anion-binding site of ClC-5 is mediated by the proton glutamate 268.

The ClC family encompasses anion channels and secondary active transporters (1–6). ClC-5 belongs to the ClC transporter branch and mediates coupled exchange of anions and protons across the biological membranes. Mutations in the *CLCN5* gene have been associated with Dent's disease (7), a kidney disorder characterized by impaired endocytosis and reduced acidification of the early endosomes (8–11).

External anions with ionic radii larger than that of Cl^- (12–14) cause partial or complete uncoupling of ClC-mediated transport. In particular, such uncoupling anions reduce the occupancy of the central anion-binding site (12), and their transport is only partially coupled to proton exchange. Coupled transport also crucially depends on a glutamate residue at the internal side of the protein, the so-called proton glutamate (Glu-268 in ClC-5). Introducing a neutral glutamine at this position in the ClC-ec1 protein uncouples anion from proton transport (15, 16). Whereas the bacterial transporter ClC-ec1 functionally tolerates various substitutions at the position corresponding to 268 (15, 16), the rather conservative E268Q substitution completely abolishes transport function in ClC-5 (13, 17). So far, no satisfactory explanation has been provided for this finding, and the role of Glu-268 in Cl^-/H^+ antiport in ClC-5 is thus still incompletely understood.

Mammalian ClC transporters display functional voltage-dependent transitions (14, 18, 19) that alter the amount of actively transporting proteins and resemble voltage-dependent gating of ion channels (14, 18). The mechanisms of these transitions are complex and include at least two different voltage-dependent processes (18). The predominantly observed depolarization-activated gating process is modulated by the type and concentration of transported substrates (18–20). Interestingly, the depolarization-induced gating in ClC-5 is associated with large gating charge movements (17). Zdebik *et al.* (13) proposed a role for the proton glutamate 268 as a modulator of this process.

A recent report showed that acidic external pH can uncouple ClC-3 transport (5). Low pH was suggested to neutralize the negative charge of another crucial glutamate residue, the so-called gating glutamate (Glu-211 in ClC-5) that plays a role in transport coupling (1, 2, 21–23). To explore whether analogous charge neutralization of the proton glutamate 268 by high internal $[H^+]$ might also result in uncoupled anion transport, we quantified transport at variable internal pH values for WT and mutant ClC-5 in which the proton glutamate 268 was mutated to histidine, cysteine, or glutamine.

EXPERIMENTAL PROCEDURES

ClC-5 Expression and Cell Culture—Expression constructs were generated by fusing the 3′ terminus of the ClC-5-encoding DNA (kindly provided by Dr. Thomas Jentsch) with a short linker (amino acid sequence TDPPVAT) and the sequence

* This work was supported by a HiLF grant from the Medical School Hannover.
[S] This article contains supplemental Figs. S1–S8 and Table S1.
[1] To whom correspondence should be addressed: Medizinische Hochschule Hannover, OE4230, Carl-Neuberg-Str. 1, D-30625 Hannover, Germany. Fax: 49-511-532-9391; E-mail: alekov.alexi@mh-hannover.de.

encoding the green fluorescent protein variant mCherry (24) into the pRcCMV vector. Point mutations were introduced using the QuikChange site-directed mutagenesis kit (Stratagene) and subsequently verified by sequencing. HEK293 and HEK293T cells were cultured in minimum Eagle's medium and DMEM (Invitrogen), respectively, supplemented with 10% fetal bovine serum (Biochrom AG). DMEM was additionally supplemented with 2 mM L-glutamine and 50 units/ml penicillin/streptomycin (Invitrogen). Cells were transfected using the calcium phosphate precipitation method (25). Cells permanently expressing the ClC-5 constructs were generated using Geneticin (G418, Invitrogen) selection and further maintained in medium supplemented with 900 μg/ml G418 (26).

Electrophysiology—Whole-cell patch clamping (27) was performed using an EPC-10 amplifier and PATCHMASTER software (HEKA). Borosilicate pipettes (Harvard Apparatus) were pulled with resistances of 0.9–2 megohms on a Sutter P-97 puller and fire-polished using a Narishige MF-900 microforge. Currents were digitized with a sampling rate of 50–100 kHz after filtering with less than one-third of the sampling rate. Series resistance compensation and capacitance cancellation were applied, resulting in <5-mV voltage error. The standard external recording solution contained 145 mM NaCl, 15 mM HEPES, 4 mM KCl, 2 mM $CaCl_2$, and 1 mM $MgCl_2$, and the internal recording solution contained 105 mM NaCl, 20 mM HEPES, 2 mM $MgCl_2$, and 5 mM EGTA. In some experiments, Cl^- was substituted on an equimolar basis using the corresponding SCN^- or $gluconate^-$ salts. At least 0.1 mM Cl^- was present in all solutions. MES buffer was used instead of HEPES for pH values below 7.4. The cysteine modification reagent sodium (2-sulfonatoethyl)methanethiosulfonate (MTSES)[2] was purchased from Toronto Research Chemicals. In all cases, 1% agar and 3 M KCl salt bridges were used to connect the Ag/AgCl electrodes to the patch-clamp solutions. Standard junction potential correction was applied when necessary (28).

Fluorescence Measurements of Intracellular pH—Fluorescence measurements of intracellular pH were performed as described previously (14). Briefly, cells were loaded with the pH-sensitive dye 2′,7′-bis(2-carboxyethyl)-5(and 6)-carboxyfluorescein (Invitrogen) at a concentration of 37.5 μM and 100 nM bafilomycin A_1 (Wako Chemicals) through the patch pipette. The buffer concentration (HEPES or MES) was 0.25 mM, and osmolarity was adjusted by raising the pipette [NaCl] to 120 mM. Measurements were performed on an inverted Olympus IX71 microscope equipped with an UPlanSApo ×60/1.35 oil immersion objective. The dye was excited sequentially at 440 and 490 nm using a Polychrome V fast-switching monochromator, and the fluorescence was detected at 530 nm using a photomultiplier tube-equipped ViewFinder III (Till Photonics). Fluorescence ratios (F_{490}/F_{440}) were calculated and converted into absolute pH using a calibration curve obtained *ex situ.*

Measurements of Membrane Capacitance—Membrane capacitance was measured with the built-in software lock-in extension of PATCHMASTER. We applied the sine-plus-DC technique (29), which uses the real and imaginary part of a sine wave signal plus the DC conductance to determine membrane capacitance, membrane conductance, and access resistance. The parameters used were as follows: sine wave at 800 Hz with 10-mV peak-to-peak amplitude and a holding potential of 0 mV. The voltage dependence of the cell capacitance was measured by changing the amplitude of the DC component of the applied voltage signal. Nonlinear capacitances were plotted against the voltage and fitted with the first derivative of a standard Boltzmann function (30) (Equations 1 and 2),

$$C(V) = \frac{\beta C_{max} e^{-\beta(V - V_{0.5})}}{(1 + e^{-\beta(V - V_{0.5})})^2} \quad \text{(Eq. 1)}$$

$$\beta = z\left(\frac{e_0 \delta}{k_B T}\right) \quad \text{(Eq. 2)}$$

where C_{max} represents the maximum nonlinear capacitance at the half-maximum voltage of activation ($V_{0.5}$), z denotes the number of elementary charges (e_0) displaced over a fraction (δ) of the membrane, k_B is the Boltzmann constant, and T is the absolute temperature.

Noise Analysis—Non-stationary noise analysis was performed as described previously (14). Briefly, an external SCN-based solution and an internal solution containing 120 mM NaI, 20 mM HEPES, 2 mM magnesium gluconate, 5 mM EGTA, and 0.1 mM NaCl were used. The data were acquired at +135 mV after filtering with a 10-kHz Butterworth filter and digitization at 100 kHz. Analysis was performed with PULSETOOLS (HEKA) using the procedures described elsewhere (31). Variances were binned, and statistical deviations were superimposed as error bars. Background noise was measured at −40 mV and subtracted. Unitary transport rates (i) and the number of transporters in the membrane (N) were determined by plotting background-corrected variances (σ^2) against the mean transport current (I) and fitting the following function to the data (Equation 3).

$$\sigma^2 = i \cdot I - \frac{I^2}{N} \quad \text{(Eq. 3)}$$

Data Analysis—Data analysis was performed using a combination of FITMASTER (HEKA), Origin (OriginLab), and Excel (Microsoft) software. All data are presented as means ± S.E.

RESULTS

External SCN^- Increases ClC-5 Currents in pH-dependent Manner—Expression in mammalian cells resulted in outwardly rectifying ClC-5 currents with amplitudes well above the background at positive potentials (Fig. 1). Exchange of external Cl^- for SCN^- resulted in strongly increased current amplitudes (Fig. 1, *A–C*). Comparison of measurements at different internal pH values revealed that this increase was much more pronounced at low internal pH (Fig. 1, *D–F*). At +135 mV, SCN^- currents were ~12 times larger than Cl^- currents at internal pH 7.4 but increased by a factor of ~50 at internal pH 6.0 (Fig. 1*G*). Control measurements with untransfected HEK293 cells in external SCN^- at low internal pH (supplemental Fig. S1) revealed negligibly small currents (~0.5-nA mean current

[2] The abbreviations used are: MTSES, sodium (2-sulfonatoethyl)methanethiosulfonate; pF, picofarad(s); fC, femtocoulomb(s) = fA × s.

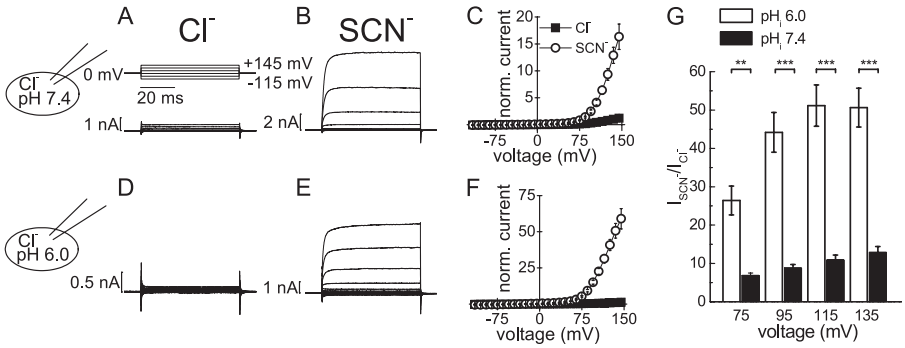

FIGURE 1. **External SCN^- increases ClC-5 current amplitudes more potently at low internal pH.** *A*, voltage protocol and representative whole-cell current traces of WT ClC-5 recorded with external and internal Cl^- at symmetric pH 7.4. *B*, whole-cell current traces from the cell depicted in *A* after perfusion with external SCN^- at pH 7.4. *D* and *E*, representative whole-cell current traces of WT ClC-5 recorded as in *A* and *B* but with internal solution at pH 6.0. *C* and *F*, averaged current-voltage curves from experiments as in *A*, *B*, *D*, and *E* depicting steady-state ClC-5 current amplitudes normalized to the ClC-5 current amplitude in external Cl^- at +135 mV and internal pH 7.4 (*C*) and pH 6.0 (*F*). *G*, increase in ClC-5 transport upon external perfusion with SCN^-. *Asterisks* indicate significant differences between measurements in internal pH 6.0 and pH 7.4: ***, $p < 0.001$; **, $p < 0.01$ (two-sample *t* test). The absolute mean currents at +135 mV in external Cl^- were 989 ± 340 pA (pH 7.4; $n = 10$) and 118 ± 19 pA (pH 6.0; $n = 8$). The absolute mean currents at +135 mV in external SCN^- were 8.3 ± 1.5 nA (pH 7.4; $n = 10$) and 5.6 ± 0.7 nA (pH 6.0; $n = 8$).

amplitude at +145 mV), in accordance with previous results (14).

Low Internal pH Values Do Not Alter Uncoupling Effect of External SCN^-—External SCN^- increases ionic currents by converting a percentage of the ClC transporters into anion channels with significantly higher unitary current amplitude (14). The pH dependence of the SCN^- effect might thus be due to a more effective uncoupling of ClC-5 at low internal pH. To test this hypothesis, we monitored the internal pH using the fluorescent pH reporter 2′,7′-bis(2-carboxyethyl)-5(and 6)-carboxyfluorescein. Cells expressing ClC-5 displayed well defined voltage-dependent intracellular alkalinization at positive potentials (Fig. 2*A*) (1, 2). At symmetric pH 7.4, however, exchanging extracellular Cl^- to SCN^- did not significantly decrease ClC-5-associated proton transport (Fig. 2, *B*, *upper panel*, and *C*). SCN^- currents were significantly larger than Cl^- currents, and the ratios of current increase and proton transport in external SCN^- normalized to the values from the same cell in external Cl^- were within the range of ~10–15 (Fig. 2*E*). Therefore, ClC-5 transport becomes uncoupled in external SCN^-, although the absolute proton transport is not significantly reduced.

At symmetric pH 6.3, ClC-5 proton transport in the same cell was even higher in external SCN^- than in external Cl^- (Fig. 2, *B*, *lower panel*, and *D*). However, the relative ratio of anion current to proton current (~10–15) (Fig. 2*F*) did not significantly differ from values obtained at internal and external pH 7.4 ($p > 0.38$ from paired *t* test).

The whole-cell patch-clamp configuration used here allows proton diffusion from the patch pipette into the measured cell. To ensure that this effect did not impair the accuracy of our results, we monitored the rate of re-acidification after each voltage pulse used to activate ClC-5 transport. This process was much slower than the ClC-5-induced alkalinization (supplemental Fig. S2) and therefore only insignificantly affected the experimentally determined transport rates (14). Moreover, in all presented measurements, SCN^- and Cl^- transport currents were compared in the same cell. Because external perfusion is not expected to change the rate of proton diffusion from the pipette solution into the cell, this strategy additionally reduces

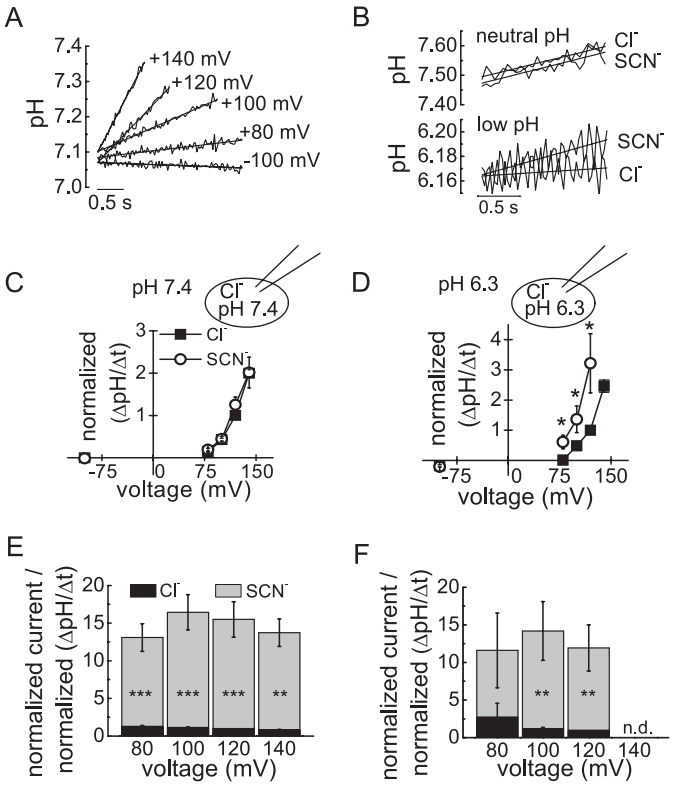

FIGURE 2. **Internal protons do not alter the uncoupling effect of external SCN^-.** *A*, representative recordings of time- and voltage-dependent internal alkalinization in a cell expressing ClC-5. *Lines* represent linear fits to the data. *B*, representative recordings of time-dependent ClC-5-mediated intracellular alkalinization at +120 mV at symmetric pH 7.4 (*upper panel*) and pH 6.3 (*lower panel*). *C* and *D*, rates of intracellular pH change in external Cl^- and SCN^- at symmetric pH 7.4 (*C*) and pH 6.3 (*D*) normalized to the value in Cl^- at +120 mV. Rates were determined using the slope of the linear fits to the data, as shown in *A*. Averaged proton flux densities at +120 mV and symmetric pH 7.4 were $9.8 \times 10^{-3} \pm 1.3 \times 10^{-3}$ $\Delta pH\ s^{-1}\ pF^{-1}$ for external Cl^- ($n = 17$) and $10.2 \times 10^{-3} \pm 1.1 \times 10^{-3}$ $\Delta pH\ s^{-1}\ pF^{-1}$ for SCN^- ($n = 14$). The corresponding averaged proton flux densities at symmetric pH 6.3 were $1.9 \times 10^{-3} \pm 0.5 \times 10^{-3}$ $\Delta pH\ s^{-1}\ pF^{-1}$ for external Cl^- ($n = 6$) and $4.3 \times 10^{-3} \pm 1.0 \times 10^{-3}$ $\Delta pH\ s^{-1}\ pF^{-1}$ for SCN^- ($n = 6$). *E* and *F*, relative transport coupling of WT ClC-5 in external Cl^- and SCN^-. Currents were normalized to +120 mV in Cl^- and divided by the normalized proton fluxes at the same voltage at symmetric pH 7.4 (*E*; $n = 6$–17) and symmetric pH 6.3 (*F*; $n = 4$–5). *Asterisks* indicate significant differences: ***, $p < 0.001$; **, $p < 0.01$; *, $p < 0.05$ (paired *t* test for non-normalized cells measured in both extracellular solutions at the same voltage). *n.d.*, not determined.

the effects of proton diffusion on the determined proportion between ClC-5 transport rates in external SCN^- and Cl^-.

Proton flux measurements were performed at symmetric internal and external pH (6.3 or 7.4). We are confident that the observed effects at pH 6.3 were not due to the low external pH or the absent transmembrane proton gradient for two reasons. First, the current increase in symmetric pH 6.3 following external SCN^- perfusion was similar to that at external pH 7.4 (supplemental Fig. S3; see also Fig. 1, *D–F*). Second, the reported identical dependence of ClC-5 on external protons in both external Cl^- and SCN^- (20) demonstrates that external protons do not interfere with the current increase following external SCN^- application.

We recently demonstrated that the dependence of the ClC-4 current amplitude on the concentration of external anions correlates with the degree of uncoupling caused by the particular anion (14). As an additional approach to test for differences in uncoupling efficiencies, we determined anion concentration dependences at pH 6.0 or 7.4 (supplemental Fig. S4) and found that they were not modified by the internal pH for Cl^- as well as for SCN^-. For both pH 6.0 and 7.4, measurements in external Cl^- provided a K_m of ~65 mM and a very shallow dependence on external [SCN^-] (supplemental Fig. S4, *C* and *D*). This indicates weaker binding affinity for uncoupling anions and is in accordance with published results (12, 14). We conclude that internal protons do not additionally uncouple ClC-5 transport.

Low Internal pH Does Not Increase ClC-5 Unitary Transport Rates—Low internal pH might increase unitary transport rates and thus augment SCN^- current amplitudes. A previous report evaluating such a possibility in external Cl^- and NO_3^- in oocytes showed unaltered ClC-5 unitary current amplitudes at different internal pH values (32). To confirm these results for external SCN^-, we applied non-stationary noise analysis to the noise associated with ClC transport. Upon membrane depolarization, the current variance and macroscopic current amplitude of ClC-5 increased with a similar time dependence (Fig. 3, *A* and *B*). Plotting the noise variance against the macroscopic current amplitude at +135 mV (Fig. 3, *C* and *D*) revealed very similar unitary current amplitudes for internal pH 6.0 and 7.4 (94.1 ± 6.3 fA ($n = 4$) and 122.8 ± 15.1 fA ($n = 3$), respectively) (Fig. 3*E*). These measurements show also that ClC-5 current variances span only the initial part of the non-stationary parabola; hence, the transport probability of ClC-5 is very low. Measurements in excised inside-out patches pulled from cells expressing ClC-5 provided similar unitary current amplitudes as obtained from whole-cell recordings (supplemental Fig. S5).

Electric Charge of Side Chain 268 Does Not Alter Depolarization-activated Voltage Gating of ClC-5—Depolarization-activated gating is the dominant voltage-dependent process in mammalian ClC transporters (18), and internal pH might modify the voltage dependence of this process. A potential protonation site accessible from the cytoplasm is the proton glutamate 268, and we thus tested neutralizing mutations of this residue. Because these mutations greatly reduce ionic currents, we employed measurements of capacitive charge movements to characterize voltage-dependent gating of ClC-5 (17).

We observed well defined voltage-dependent gating currents in WT ClC-5 and in the two proton glutamate mutations

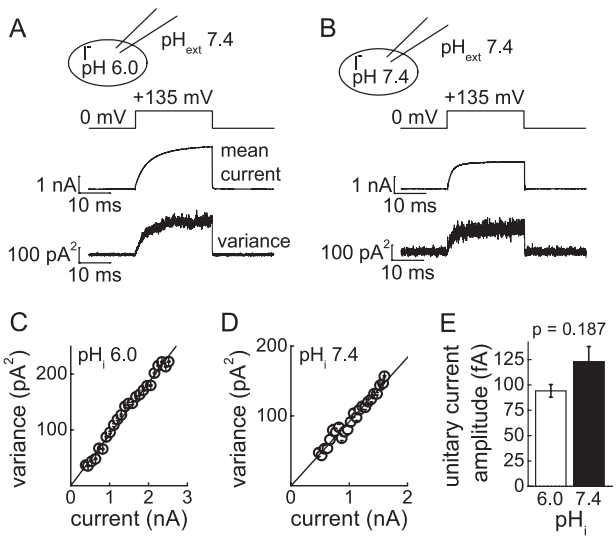

FIGURE 3. **Internal pH does not change unitary current amplitudes of ClC-5 in external SCN^-.** *A* and *B*, voltage protocols, representative ClC-5 mean currents, and variances used for non-stationary noise analysis at internal pH 6.0 (*A*) and pH 7.4 (*B*). Measurements were performed in external SCN-based solution (pH 7.4) and internal iodide-based solutions. Averaged mean steady-state currents were 2.9 ± 0.3 nA ($n = 4$) and 2.7 ± 0.5 nA ($n = 3$) at internal pH 6.0 and 7.4, respectively, with mean variances of 222 ± 9 and 237 ± 54 pA^2. *C* and *D*, representative variance-current plots for the cells shown in *A* and *B*. *Lines* represent parabolic fits of Equation 3 to the data. *E*, mean unitary current amplitudes for ClC-5 at internal pH 6.0 and 7.4. The *p* value shows the result of a two-sample *t* test.

E268H and E268Q (Fig. 4, *A–C*). To quantify the voltage dependence of ClC-5 with high accuracy, we monitored nonlinear membrane capacitances by performing admittance measurements on ClC-5-expressing cells using the built-in lock-in amplifier of the EPC-10 amplifier (29). These measurements revealed large bell-shaped capacitance changes (Fig. 4, *D–F*). The voltage dependence of these changes could be well fitted with the first derivative from the standard Boltzmann equation (30). The maximum of the capacitance curve at symmetric pH is at approximately +160 mV, and the slope gives an estimate of approximately $-1e_0$ for the electric charge associated with the gating process (Fig. 4, *D–F*, and supplemental Table S1). These values report on the voltage dependence of the depolarization-activated gate and correspond to values previously reported for ClC-5 (17), ClC-4 (18), and ClC-7 (19).

We expected that glutamate and histidine side chains at position 268 would become protonated and correspondingly neutral and positively charged at low internal pH. In general, the electric charge of a glutamine side chain should not be altered. In the case that the proton glutamate 268 is involved in the depolarization-activated voltage sensing, one would expect dramatic changes in the voltage dependence of the activation of ClC-5. In contrast, all of these proteins showed similar behavior with respect to the observed gating currents (Fig. 4, *D–F*). Measurements at different internal pH values revealed an almost identical half-maximum voltage of activation for all tested constructs (Fig. 4, *G–I*). As an additional test, we measured steady-state open probabilities of ClC-5 in external SCN^- at different internal pH values using tail current analysis (supplemental Fig. S6) (18). However, the detected changes cannot account for the larger current amplitudes in external SCN^-.

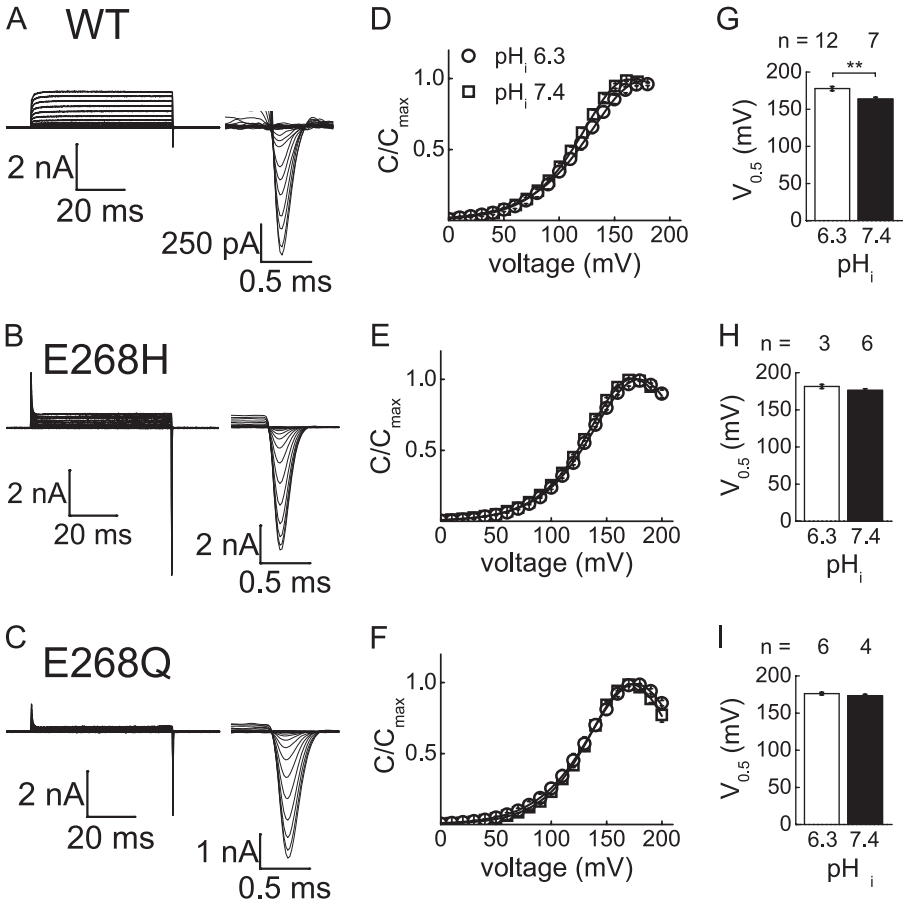

FIGURE 4. **Gating charge movements and nonlinear capacitances of ClC-5.** *A–C*, representative current recordings from WT ClC-5 and mutants E268H and E268Q in internal and external Cl^- solutions at pH 7.4 at voltage steps from −115 to +165 mV. To eliminate linear capacitance peaks, *p/N* leak subtraction was applied. The *insets* depict enlarged gating charge movements at the end of the voltage pulses (off-charge). The mean ClC-5 currents at +165 mV were 2.9 ± 0.5 nA (pH 7.4) and 2.9 ± 0.8 nA (pH 6.3) for WT ClC-5, 0.8 ± 0.2 nA (pH 7.4) and 0.9 ± 0.2 nA (pH 6.3) for E268H ClC-5, and 0.2 ± 0.1 nA (pH 7.4) and 0.2 ± 0.1 nA (pH 6.3) for E268Q ClC-5. *D–F*, normalized nonlinear capacitances for WT, E268H, and E268Q ClC-5 at internal pH 6.3 and 7.4 and in external solution with reduced [Cl^-] (500 μM, pH 7.4). *Lines* represent fits of the first derivative of a Boltzmann function (Equation 1) to the data with fit parameters shown in supplemental Table S1. Averaged maximum nonlinear capacitances at different internal pH values were 1.7 ± 0.3 pF (pH 6.3) and 3.8 ± 1.2 pF (pH 7.4) for WT ClC-5, 1.3 ± 0.6 pF (pH 6.3) and 8.2 ± 2.7 pF (pH 7.4) for E268H ClC-5, and 3.6 ± 0.7 pF (pH 6.3) and 2.6 ± 0.4 pF (pH 7.4) for E268Q ClC-5. *G–I*, mean half-maximum voltage of activation ($V_{0.5}$; Equation 1) of WT, E268H, and E268Q ClC-5, respectively. *Asterisks* indicate significant difference from a two-sample *t* test: **, $p < 0.01$.

We conclude that the charge of the proton glutamate 268 of ClC-5 is not directly involved in voltage sensing during depolarization-induced activation.

Proton glutamate 268 Is Exposed to Intracellular Solution and Directly Regulates Transport Probability and Nonlinear Capacitances in ClC-5—To test whether position 268 is accessible from the aqueous solution, we introduced a cysteine mutation at this position and tested whether the cysteine side chain can be reacted with sulfhydryl reagents. Covalently linking a chemical compound with a negative charge permits direct monitoring of the effects associated with changes of the charge at position 268. Dynamic changes of the electric charge are expected to take place during the protonation-deprotonation cycle accompanying ClC transport (23). The ClC-5 mutant E268C exhibited very small transport currents but large gating currents before modification (Fig. 5*B* and supplemental Fig. S7). Application of the negatively charged and protonatable MTSES in the patch pipette increased transport currents in a time-dependent fashion (Fig. 5, *B* and *C*). The amplitudes of the gating currents decreased with the same time dependence as the current increase (Fig. 5*E*). Application of MTSES to cells expressing mutation E268Q did not result in any time-dependent changes.[3] Therefore, the effects observed in mutant E268C are due to the modification of the cysteine side chain. Because neither coupling nor unitary current amplitudes were altered upon partial neutralization of the negative charge of Glu-268 by low internal pH, we conclude that the small transport currents of ClC-5 mutation E268C reflect low transport probability that increases upon modification with MTSES. In addition, the inversely proportional correlation between nonlinear capacitance and transport currents in ClC-5 (Fig. 5, *B–D*) indicates that the observed large gating currents originate from incomplete transport cycles.

Titratable Residue at Position 268 Is Required for ClC-5 Transport—Because gating currents are based on incomplete transport cycles and ionic currents on complete cycles or uncoupled currents, the relative amount of incomplete transport cycles can be quantified by normalizing the ClC-5 nonlinear capacitance (*C*) to the transport current (*I*) measured in the

[3] M. Grieschat and A. K. Alekov, unpublished data.

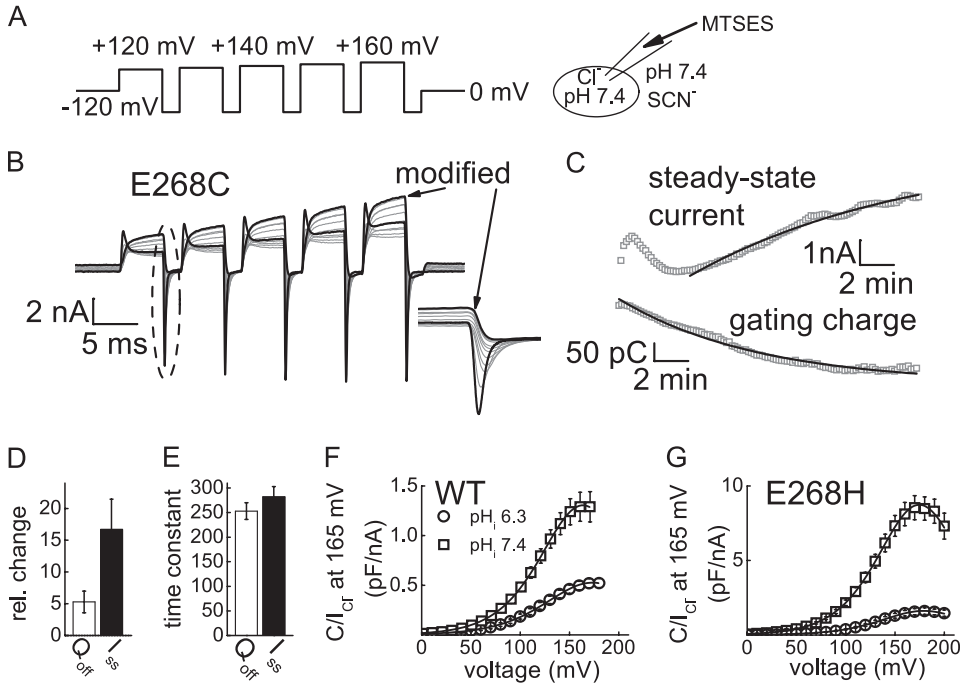

FIGURE 5. **Proton glutamate 268 modulates transport probability and nonlinear capacitances of ClC-5.** *A*, voltage protocol and ionic conditions for the modification experiment depicted in *B*. *B*, representative traces showing the modification of the proton glutamate mutation E268C with the negatively charged reagent MTSES. MTSES was added to the pipette solution at a concentration of 2.5 mM, and the *p/N* leak-subtracted E268C currents in external SCN^- (pH 7.4) were monitored for 10 min immediately after obtaining whole-cell configuration. The *inset* depicts enlarged ClC-5 gating charge movements. *C*, time course of the current amplitudes measured at the end of the pulses at +160 mV (*upper panel*) and the gating charges (*lower panel*) obtained by integration of the off-gating currents at the same potential. *Lines* represent monoexponential fits to the data. *D*, relative decrease and increase after modification for the off-gating charge (Q_{off}) and the steady-state current (I_{ss}) at +160 mV. The average ClC-5 currents at +160 mV before and after MTSES modification were 1.1 ± 0.7 and 3.1 ± 1.1 nA ($n = 4$), respectively. The average off-gating charges after the +160-mV prepulse before and after MTSES modification were 880 ± 380 and 68 ± 30 fC ($n = 4$), respectively. *E*, mean time constants for modification of the off-gating charge and the steady-state current by MTSES determined as depicted in *C* ($n = 4$; $p = 0.34$). *F* and *G*, nonlinear capacitances of WT ClC-5 (*F*) and E268H ClC-5 (*G*) at internal pH 6.3 and 7.4 from Fig. 4 were normalized to the steady-state transport current in the same cell at +165 mV at standard external $[Cl^-]$. *Lines* represent fits of the first derivative of the Boltzmann function to the data (Equation 1).

same cell. Capacitance and current amplitudes both depend on the number of ClC-5 transporters in the membrane (N), the probability for the completed or incomplete transport cycles (P_C and P_{NC}), and the unitary current (i) or unitary gating charge (q), respectively (Equations 4 and 5).

$$C = N \cdot P_{NC} \cdot q \quad \text{(Eq. 4)}$$

$$I = N \cdot P_C \cdot i \quad \text{(Eq. 5)}$$

Because the number of transporters and the unitary transport rate (charge) are invariants, the ratio between nonlinear capacitance and transport current (dividing Equation 4 by Equation 5) provides the relative probabilities of incomplete and completed transport cycles (P_{NC}/P_C). This ratio is smaller at lower internal pH, indicating reduced probability of incomplete and increased probability of full transport-associated cycles (Fig. 5*F*). For ClC-5 mutation E268H, the probability of incomplete transport cycles is much higher, but the internal pH has similar effects on the current/capacitance proportion (Fig. 5*G*). These results suggest that for the completion of the ClC-5 transport cycle, the charge of the amino acid side chain at position 268 is not critical; more significant is its ability to accept protonation.

Internal Protons Modify ClC-5 by Protonating Gating Glutamate 211 at Central Anion-binding Site—The recently solved crystal structure of eukaryotic cmCLC (23) provides a framework for interpreting the effects of internal protons. This intermediate-state structure captures the gating glutamate of cmCLC bound to the central anion-binding site and thereby occluding the anion permeation pathway. Occlusion of the central binding site would abolish both coupled and uncoupled ClC-5 transport. Therefore, on the basis of the increased transport probability of these two modes (Figs. 1 and 2), we speculated that internal protons might reach this site and destabilize the binding of the gating glutamate there.

To test this hypothesis, we investigated the effects of internal protons on the E211C mutant, in which the gating glutamate (22) is substituted with cysteine. This maneuver results in a neutral side chain and is expected to relocate the gating glutamate to the extracellular solution (22, 23). We note that a cysteine side chain also could be deprotonated and probably partially negatively charged. However, this mutation changed the general properties of ClC-5 very similarly to a glutamine mutation at the same position (1, 2, 13). In particular, the coupled proton transport, transport rectification in symmetric Cl^-, and gating charge movements were abolished.[3] Therefore, we assumed that the cysteine side chain is electrically neutral under our experimental conditions for most of the time. E211C greatly reduced the sensitivity of ClC-5 to internal protons (Fig. 6*A*). Superfusion with external SCN^- led to a strong increase (~30-fold) in macroscopic currents compared with measurements in external Cl^- at internal pH 6.0 and 7.4 (Fig. 6, *C*, *E*, and

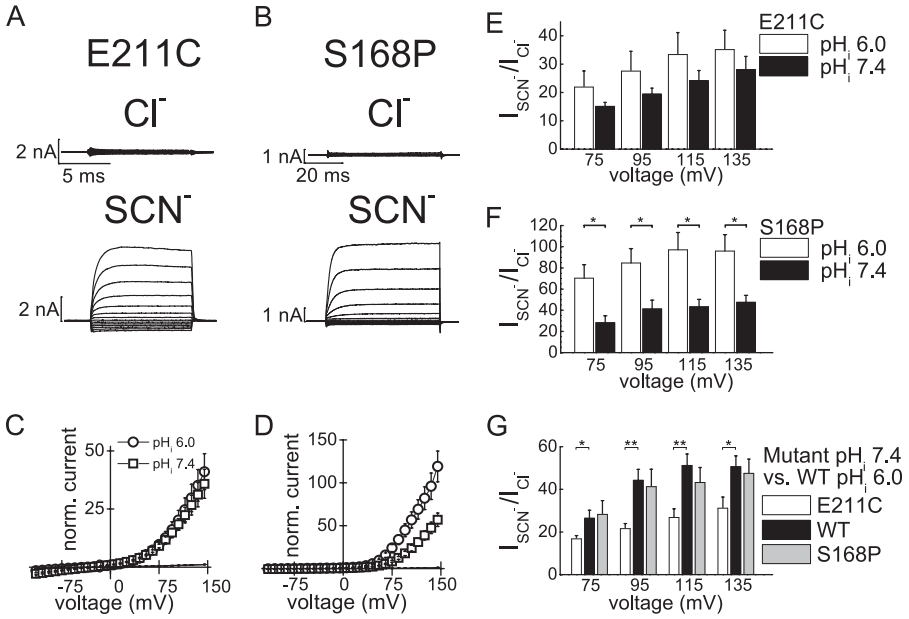

FIGURE 6. **SCN-mediated current increase is modulated by mutations E211C and S168P.** *A* and *B*, representative whole-cell recordings of cells expressing the gating glutamate mutant E211C (*A*) and mutant S168P at the central anion-binding site (*B*) at symmetric pH 7.4 and voltage steps from −115 to +145 mV. The same cell was superfused externally with Cl^- or SCN^-. *C* and *D*, current-voltage curves for mutations E211C (*C*) and S168P (*D*) in acidic and neutral internal chloride-based solutions and external Cl^- or SCN^-. SCN^- currents are indicated by symbols, and the small Cl^- currents are shown as *lines* ($n = 4$ for E211C at pH 6.0 and 7.4 and $n = 7$ and 8 for S168P at pH 6.0 and 7.4). Mean currents of E211C ClC-5 at +135 mV and different internal pH values were 138 ± 46 pA (pH 6.0) and 170 ± 57 pA (pH 7.4) in external Cl^- and 4.7 ± 2.1 nA (pH 6.0) and 4.4 ± 1.1 nA (pH 7.4) in external SCN^-. Mean currents for S168P in Cl^- at internal pH 6.0 and 7.4 were 76 ± 12 and 80 ± 12 pA, respectively, and those in external SCN^- were 6.0 ± 0.6 and 3.5 ± 0.4 nA, respectively. *E* and *F*, summary data for the SCN^- current increase at selected voltages. *Asterisks* indicate significant differences between measurements in internal pH 6.0 and pH 7.4: *, $p < 0.05$ (two-sample *t* test). *G*, comparison of the effects of internal pH 6.0 and external SCN^- on WT ClC-5 (data from Fig. 1*G*) with the effects of internal pH 7.4 and external SCN^- on ClC-5 mutants E211C and S168P (data from *E* and *F*). *Asterisks* indicate significant differences in comparison with WT ClC-5: **, $p < 0.01$; *, $p < 0.05$.

G). This ratio resembles the behavior of WT ClC-5 at acidic internal pH values (Fig. 1).

A mutation causing substitution of Ser-168 at the central anion-binding site with proline (S168P) is expected to weaken the binding of Cl^- to this site (32, 33). Because anions compete with the gating glutamate, S168P is expected also to weaken the binding of the gating glutamate to this site. For S168P ClC-5, superfusion with external SCN^- at internal pH 7.4 led to ~50-fold increase in macroscopic ClC-5 currents compared with external Cl^- (Fig. 6, *B*, *D*, *F*, and *G*). This ratio resembles the behavior of WT ClC-5 at low internal pH (Fig. 1). A high internal proton concentration additionally increased transport (Fig. 6, *D* and *F*); however, the increase was smaller compared with WT ClC-5 (~1.5-fold for S168P ClC-5 and ~4-fold for WT ClC-5). These findings indicate that a generally reduced occupancy of the central anion-binding site results in increased transport probability in external SCN^-.

DISCUSSION

We have quantified the effects of internal protons on transport and gating of the anion/proton exchanger ClC-5. We were able to demonstrate that internal acidification increases coupled anion/proton as well as uncoupled anion transport. ClC-5 exhibits voltage-dependent gating in both functional modes (Fig. 1). However, the depolarization-activated gating process was not altered by low internal pH values (Fig. 4 and supplemental Fig. S6). We thus conclude that internal protons alter an additional distinct gating process that regulates the transport probability of both transport modes. The effects of internal protons, as well of mutations, neutralizing the proton glutamate 268 (Figs. 1–5) provide evidence that the observed effects are due to protonation of the gating glutamate 211. We have furthermore demonstrated that mutation S168P (Fig. 6), which reduces anion occupancy of the central binding site, affects the protonation of the gating glutamate. These findings support the notion that protonation of the gating glutamate bound to the central anion-binding site in an intermediate state is the basis for the observed effects (see scheme in Fig. 7).

Our results differ from earlier reports showing decreased proton transport by ClC transporters upon external anion exchange of Cl^- for SCN^-. For ClC-5, earlier experiments were performed in *Xenopus laevis* oocytes (13) using two-electrode voltage clamping. Because this technique does not allow the precise control of the concentration of intracellular anions and because internal anions significantly modify ClC transport (17, 18),[3] the different outcomes of the two studies are most likely due to variation in the experimental strategy. For ClC-4 (14), we used the same experimental strategies as in the present study and found decreased proton currents for ClC-4 and identical or even increased proton currents for ClC-5 upon SCN^- application (Fig. 2). We conclude that there are isoform-specific differences in the effects of uncoupling ions on diverse ClC transporters.

Non-stationary noise analysis revealed further differences between ClC-4 and ClC-5. Uncoupled transport dominates measured currents in external SCN^- (Fig. 1), and noise analysis thus reports the properties of this specific mode. We found

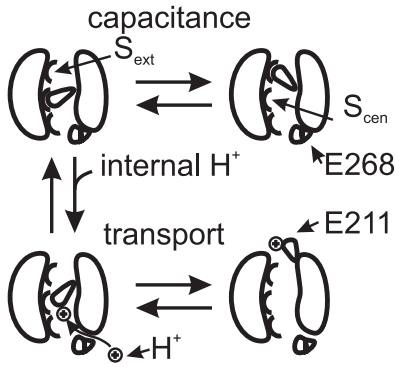

FIGURE 7. **Hypothetical model representing protonation of gating glutamate at central anion-binding site.** When the gating glutamate 211 is in its negative unprotonated form, it can swing between the central (S_{cen}) and external (S_{ext}) anion-binding sites. At these positions, the gating glutamate 211 occludes the anion permeation pathway, and ClC-5 is not mediating ion transport. The motion is associated with the changes in nonlinear capacitance observed in ClC-5. Protonation via a pathway including the proton glutamate 268 allows reallocation of the gating glutamate 211 toward the extracellular lumen and transport. No capacitance changes are observed upon depolarization in this case. Internal pH and mutations of the proton glutamate 268 will modulate the distribution between transporting and "capacitive" ClC-5.

that, under our experimental conditions, the transport probability of ClC-5 is very low (Fig. 3 and supplemental Fig. S5). This is in clear contrast to ClC-4, which displays a transport probability of ~50% (14). ClC-4 and ClC-5 thus differ also in their maximum transport probabilities.

Unitary current amplitudes of ClC-5 in external SCN^- were independent of the internal pH, in agreement with earlier results reported for external NO_3^- (32). The ~4-fold increase in the SCN^- current amplitudes at pH 6.0 compared with pH 7.4 (Fig. 1) suggests that external SCN^- increases the overall transport probability of ClC-5. This is consistent with the previously detected larger number of active ClC-4 transporters upon superfusion with external SCN^- (14). The existence of gating processes in mammalian ClC transporters is already well established (14, 17–19). Similar to ClC-4 (18), ClC-5 currents are dominated by a prominent depolarization-activated process (Figs. 1 and 4 and supplemental Fig. S6). However, the voltage dependence of this process at different internal pH values (Fig. 4 and supplemental Fig. S6) suggests that it is not responsible for the synergism between internal protons and external SCN^-. Depolarization-activated gating of ClC-4 is analogously unaffected by internal protons (18), supporting the idea that the transport probability of mammalian ClC transporters is regulated also by an additional distinct gating process. We have already demonstrated the existence of such a process at negative transmembrane voltages in ClC-4 (18). The data presented here serve as additional evidence for the presence of complex voltage- and substrate-dependent gating in mammalian ClC transporters.

The depolarization-induced activation of the transporter-type ClC protein ClC-5 is associated with large voltage-dependent charge movements (17). We have shown here that the observed gating currents result from an increased electric capacitance associated with the depolarization-induced activation of ClC-5 (Fig. 4). The nonlinear capacitance of ClC-5 resembles the features of prestin, the motor protein of the outer hair cells (30). It represents a bell-shaped curve and can be mathematically described as movement of a charged particle in the membrane electric field. In ClC-5, the amplitudes of the gating charge movements and nonlinear capacitance are inversely proportional to the transport amplitude (Figs. 4 and 5). Therefore, we conclude that the observed nonlinear capacitance originates from incomplete ClC-5 transport cycles. This aspect resembles the so-called presteady-state transporter currents described for a variety of neurotransmitter, amino acid, or sugar transporters (34–36). In these transporters, presteady-state currents occur when the substrate is absent but disappear in the presence of saturating amounts of substrate. In ClC-5, the nonlinear capacitance increases at higher pH and when the proton glutamate 268 is mutated (Figs. 4 and 5). This suggests an inversely proportional dependence between the effective injection of protons into the transporting machinery of the protein and the gating charge moved during ClC-5 activation.

We constructed a (hypothetical) model (Fig. 7) based on published crystal structures of ClC transporters. For simplicity, we omitted in this model possible steps depicting binding and translocation of Cl^- (supplemental Fig. S8). However, it should be noted that nonlinear capacitance is observed also in the absence of external permeable anions, whereas the experimentally observed transport naturally requires the presence of such anions. The simple model (Fig. 7) is in full agreement with our experimental data. The pH independence of the E211C ClC-5 SCN^- currents (Fig. 6) suggests that protons increase the transport probability of ClC-5 by neutralizing the negative charge of the gating glutamate. Proton transport by ClC transporters utilizes movement of this glutamate side chain between different positions (23), the central and external anion-binding sites. The gating glutamate can occupy both sites in its deprotonated negatively charged form, and the change in position between these two sites is then responsible for the observed nonlinear gating charge movements. However, reallocation of the gating glutamate to the external solution, required for anion transport, is only possible after protonation. Movements of the gating glutamate in the absence of proton delivery will thus result in incomplete transport cycles and high nonlinear capacitance changes in ClC-5 (Figs. 4 and 5). Coupled transport requires protons to move from the proton glutamate 268 to the gating glutamate 211. Therefore, mutations of the proton glutamate 268 will either modify the capacitance/transport proportion (E268H) or abolish transport (E268Q) (Fig. 4). The model also predicts that internal protons and mutations of the proton glutamate do not shift the voltage dependence of the nonlinear capacitance of ClC-5 (Fig. 4). S168P should also facilitate the reallocation of the gating glutamate and shift the activation of ClC-5 toward less depolarized potentials, which is indeed the case.[3] The proposed model is also in full agreement with the observed restoration of WT behavior after reacting a negative reagent with Cys-268 (Fig. 5). The eukaryotic cmCLC (23) and bacterial ClC-ec1 (15) proteins are both able to support transport without proton glutamate. In contrast, the ClC-5 mutation E268Q is non-transporting (Fig. 4). Stronger binding of the gating glutamate 211 in ClC-5 when the side chain is not protonated might explain this effect. Such more restrictive requirements would assure stricter thermodynamic coupling of anion

and proton transport in mammalian ClC proteins and explain why mammalian ClC transporters are still able to perform partially coupled antiport of protons in external SCN^-.

Acknowledgments—We thank Ch. Fahlke, M. Fischer, J. P. Machtens, and G. Stölting for critical reading of the manuscript.

REFERENCES

1. Scheel, O., Zdebik, A. A., Lourdel, S., and Jentsch, T. J. (2005) Voltage-dependent electrogenic chloride/proton exchange by endosomal CLC proteins. *Nature* **436,** 424–427
2. Picollo, A., and Pusch, M. (2005) Chloride/proton antiporter activity of mammalian CLC proteins ClC-4 and ClC-5. *Nature* **436,** 420–423
3. De Angeli, A., Monachello, D., Ephritikhine, G., Frachisse, J. M., Thomine, S., Gambale, F., and Barbier-Brygoo, H. (2006) The nitrate/proton antiporter AtCLCa mediates nitrate accumulation in plant vacuoles. *Nature* **442,** 939–942
4. Graves, A. R., Curran, P. K., Smith, C. L., and Mindell, J. A. (2008) The Cl^-/H^+ antiporter ClC-7 is the primary chloride permeation pathway in lysosomes. *Nature* **453,** 788–792
5. Matsuda, J. J., Filali, M. S., Collins, M. M., Volk, K. A., and Lamb, F. S. (2010) The ClC-3 Cl^-/H^+ antiporter becomes uncoupled at low extracellular pH. *J. Biol. Chem.* **285,** 2569–2579
6. Neagoe, I., Stauber, T., Fidzinski, P., Bergsdorf, E. Y., and Jentsch, T. J. (2010) The late endosomal ClC-6 mediates proton/chloride countertransport in heterologous plasma membrane expression. *J. Biol. Chem.* **285,** 21689–21697
7. Lloyd, S. E., Pearce, S. H., Fisher, S. E., Steinmeyer, K., Schwappach, B., Scheinman, S. J., Harding, B., Bolino, A., Devoto, M., Goodyer, P., Rigden, S. P., Wrong, O., Jentsch, T. J., Craig, I. W., and Thakker, R. V. (1996) A common molecular basis for three inherited kidney stone diseases. *Nature* **379,** 445–449
8. Piwon, N., Günther, W., Schwake, M., Bösl, M. R., and Jentsch, T. J. (2000) ClC-5 Cl^--channel disruption impairs endocytosis in a mouse model for Dent disease. *Nature* **408,** 369–373
9. Hara-Chikuma, M., Wang, Y., Guggino, S. E., Guggino, W. B., and Verkman, A. S. (2005) Impaired acidification in early endosomes of ClC-5-deficient proximal tubule. *Biochem. Biophys. Res. Commun.* **329,** 941–946
10. Smith, A. J., Reed, A. A., Loh, N. Y., Thakker, R. V., and Lippiat, J. D. (2009) Characterization of Dent disease mutations of ClC-5 reveals a correlation between functional and cell biological consequences and protein structure. *Am. J. Physiol. Renal Physiol.* **296,** F390–F397
11. Novarino, G., Weinert, S., Rickheit, G., and Jentsch, T. J. (2010) Endosomal chloride/proton exchange rather than chloride conductance is crucial for renal endocytosis. *Science* **328,** 1398–1401
12. Nguitragool, W., and Miller, C. (2006) Uncoupling of a CLC Cl^-/H^+ exchange transporter by polyatomic anions. *J. Mol. Biol.* **362,** 682–690
13. Zdebik, A. A., Zifarelli, G., Bergsdorf, E. Y., Soliani, P., Scheel, O., Jentsch, T. J., and Pusch, M. (2008) Determinants of anion/proton coupling in mammalian endosomal CLC proteins. *J. Biol. Chem.* **283,** 4219–4227
14. Alekov, A. K., and Fahlke, Ch. (2009) Channel-like slippage modes in the human anion/proton exchanger ClC-4. *J. Gen. Physiol.* **133,** 485–496
15. Accardi, A., Walden, M., Nguitragool, W., Jayaram, H., Williams, C., and Miller, C. (2005) Separate ion pathways in a Cl^-/H^+ exchanger. *J. Gen. Physiol.* **126,** 563–570
16. Lim, H. H., and Miller, C. (2009) Intracellular proton-transfer mutants in a CLC Cl^-/H^+ exchanger. *J. Gen. Physiol.* **133,** 131–138
17. Smith, A. J., and Lippiat, J. D. (2010) Voltage-dependent charge movement associated with activation of the CLC-5 $2Cl^-/1H^+$ exchanger. *FASEB J.* **24,** 3696–3705
18. Orhan, G., Fahlke, Ch., and Alekov, A. K. (2011) Anion- and proton-dependent gating of CIC-4 anion/proton transporter under uncoupling conditions. *Biophys. J.* **100,** 1233–1241
19. Leisle, L., Ludwig, C. F., Wagner, F. A., Jentsch, T. J., and Stauber, T. (2011) ClC-7 is a slowly voltage-gated $2Cl^-/1H^+$ exchanger and requires Ostm1 for transport activity. *EMBO J.* **30,** 2140–2152
20. Picollo, A., Malvezzi, M., and Accardi, A. (2010) Proton block of the CLC-5 Cl^-/H^+ exchanger. *J. Gen. Physiol.* **135,** 653–659
21. Accardi, A., and Miller, C. (2004) Secondary active transport mediated by a prokaryotic homolog of ClC Cl^- channels. *Nature* **427,** 803–807
22. Dutzler, R., Campbell, E. B., and MacKinnon, R. (2003) Gating the selectivity filter in ClC chloride channels. *Science* **300,** 108–112
23. Feng, L., Campbell, E. B., Hsiung, Y., and MacKinnon, R. (2010) Structure of a eukaryotic CLC transporter defines an intermediate state in the transport cycle. *Science* **330,** 635–641
24. Shaner, N. C., Campbell, R. E., Steinbach, P. A., Giepmans, B. N., Palmer, A. E., and Tsien, R. Y. (2004) Improved monomeric red, orange, and yellow fluorescent proteins derived from *Discosoma* sp. red fluorescent protein. *Nat. Biotechnol.* **22,** 1567–1572
25. Graham, F. L., and van der Eb, A. J. (1973) A new technique for the assay of infectivity of human adenovirus 5 DNA. *Virology* **52,** 456–467
26. Hebeisen, S., Heidtmann, H., Cosmelli, D., Gonzalez, C., Poser, B., Latorre, R., Alvarez, O., and Fahlke, Ch. (2003) Anion permeation in human ClC-4 channels. *Biophys. J.* **84,** 2306–2318
27. Hamill, O. P., Marty, A., Neher, E., Sakmann, B., and Sigworth, F. J. (1981) Improved patch-clamp techniques for high-resolution current recording from cells and cell-free membrane patches. *Pflugers Arch.* **391,** 85–100
28. Barry, P. H. (1994) JPCalc, a software package for calculating liquid junction potential corrections in patch-clamp, intracellular, epithelial, and bilayer measurements and for correcting junction potential measurements. *J. Neurosci. Methods* **51,** 107–116
29. Gillis, K. D. (2000) Admittance-based measurement of membrane capacitance using the EPC-9 patch-clamp amplifier. *Pflugers Arch.* **439,** 655–664
30. Santos-Sacchi, J. (1991) Reversible inhibition of voltage-dependent outer hair cell motility and capacitance. *J. Neurosci.* **11,** 3096–3110
31. Heinemann, S. H., and Conti, F. (1992) Non-stationary noise analysis and application to patch-clamp recordings. *Methods Enzymol.* **207,** 131–148
32. Zifarelli, G., and Pusch, M. (2009) Conversion of the $2Cl^-/1H^+$ antiporter ClC-5 in a NO_3^-/H^+ antiporter by a single point mutation. *EMBO J.* **28,** 175–182
33. Picollo, A., Malvezzi, M., Houtman, J. C., and Accardi, A. (2009) Basis of substrate binding and conservation of selectivity in the CLC family of channels and transporters. *Nat. Struct. Mol. Biol.* **16,** 1294–1301
34. Bossi, E., Centinaio, E., Castagna, M., Giovannardi, S., Vincenti, S., Sacchi, V. F., and Peres, A. (1999) Ion binding and permeation through the lepidopteran amino acid transporter KAAT1 expressed in *Xenopus* oocytes. *J. Physiol.* **515,** 729–742
35. Hazama, A., Loo, D. D., and Wright, E. M. (1997) Presteady-state currents of the rabbit Na^+/glucose cotransporter (SGLT1). *J. Membr. Biol.* **155,** 175–186
36. Mager, S., Naeve, J., Quick, M., Labarca, C., Davidson, N., and Lester, H. A. (1993) Steady states, charge movements, and rates for a cloned GABA transporter expressed in *Xenopus* oocytes. *Neuron* **10,** 177–188